KSTLE International Journal, Vol. 3, No. 1, June 2002, pp. 60-67

Analysis of Sliding/Impacting Wear in Tube to Convex Spring Contact and Relevant Contact Problem

Hyung-Kyu Kim†, Young-Ho Lee, Sung-Pil Heo, Youn-Ho Jung, Jae-Wook Ha*, Seock-Sam Kim* and Kyeong-Lak Jeon**

Korea Atomic Energy Research Institute 150 Dukjin-dong, Yusong-ku Taejon, 305-353 Korea
**School of Mechanical Engineering, Kyungpook National University, 1370 Sankyuk-dong, Puk-ku Taegu, 702-701 Korea*
***KEPCO Nuclear Fuel Co., LTD. 150 Dukjin-dong, Yusong-ku Taejon, 305-353 Korea*

Abstract : Wear on the tube-to-spring contact is investigated experimentally. The vibration of the tube causes the wear while the springs support it. As for the supporting conditions, the contacting normal force of 5 N, 0 N and the gap of 0.1 mm are applied. The gap condition is for considering the influence of simultaneous impacting and sliding on wear. The wear volume and depth decreases in the order of the 5 N, 0 N and the gap conditions. This is explained from the contact geometry of the spring, which is convex of smooth contour. The contact shear force is regarded smaller in the case of the gap existence compared with the other conditions. The wear mechanism is considered from SEM observation of the worn surface. The variation of the normal contact traction is analysed using the finite element analysis to estimate the slip displacement range on the contact with consulting the fretting map.

Keywords : Tube to spring contact, thin strip spring, convex contour, impact and sliding wear, contact traction

Introduction

Fretting damage, occurring due to the relative slip displacement of a small amplitude between the contacting bodies, often causes premature material failure such as wear, fatigue cracking or both of them. Design life of a component or a structure cannot be reached due to the fretting damage, which is the primary reason of the study on fretting. Since the fretting damage occurs on the contact surface, it is important to analyze the contact phenomenon. In the analysis of that, included is the contact condition such as contact shape and contact force. In general, the contacting part is designed to keep sound fastening or supporting during service. However, it can be loosened as the service life increases due to undesirable vibration, environmental effect etc. A gap may be formed resultantly on the contact. Once a gap exists on the contact, the failure mechanism can be changed and the added impact force may accelerate the failure. This is the major concern of the present paper.

A tube supported by a set of thin strip springs is considered here. When the tube vibrates, wear occurs on the contact between the springs and the tube, that is the case of nuclear fuel rod and spacer grid spring during reactor operation. The intrinsic function of the spring is to support the fuel rod to locate in a proper position inside the fuel assembly. Due to the thermal as well as the irradiation effect, the characteristic of the spacer grid spring is to be degraded. Insufficient support can be resulted as the residence time inside the reactor increases. Even, a gap is sometimes formed between the rod and the spring. When a gap is formed, the amplitude of the fuel rod vibration due to the coolant flow increases further, which usually results in severe wear on the rod. The fuel rod is slipped down when the gap is formed. From the viewpoint of fuel mechanical designer, it must be primary concern to design the spring of intact support capability even in the severe reactor condition. Therefore, it is important to investigate the influence of the supporting condition on the fuel rod wear. Since the wear on the rod is affected by the contact shape of the spring (i.e., the end profile of the spring which is in contact with rod surface), it can be one of the solutions to improve the contact shape of the spring to control the wear.

In this research, a tube contact with a spring of convex contour is investigated experimentally. In the experiment, supporting condition is varied as a positive contact force of 5 N, 0 N (termed "*just contact*" *ad hoc*) and negative contact of 0.1 mm gap. Wear volume and depth on the tube are examined to investigate the influence of the contact condition. The wear mechanism is also investigated from the scanning electron microscopic (SEM) view of the worn surface. In addition to the experimental analysis, the contact traction is analyzed using the finite element analysis. This theoretical analysis is carried out to explain the shape of the wear scar. The variation of the traction found during the contact force increase is discussed.

†Corresponding author; Tel: 82-42-868-2111, Fax: 82-42-863-0565
E-mail: hkkim1@kaeri.re.kr

Table 1. Mechanical properties of the spring material

Mechanical properties (at room temperature)		
Yield strength (0.2% offset)	Elastic Modulus	Poissons Ratio
344.3 MPa	180.332 GPa	0.294

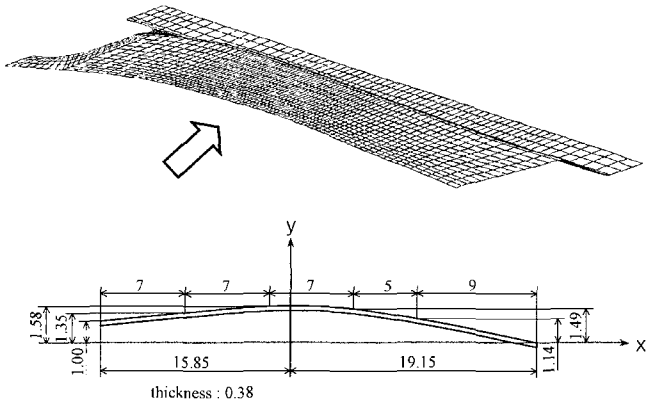

Fig. 1. Section view of the spring experimented (unit: mm).

Experiment

Specimen

The material of the tube and the strip spring specimen is the same, zirconium alloy, which is used for light-water nuclear fuel. The mechanical properties of the material are listed in Table 1. The diameter and the thickness of the tube specimen are 9.5 mm and 0.6 mm, respectively. A spring specimen is fabricated by pressing the strip of 0.38 mm. As given in Fig. 1, the cross-sectional view (along tube axis) of the spring specimen is convex. The spring has convex contour also in transverse direction. Therefore, the tube starts to contact with the spring at the highest point. As the force increases, the spring deforms to be flat on the contact region corresponding to the tube surface. Simultaneously, circular arcs of different radii are formed outside the contact region while the force is applied. The length and the width of the contact region expand as the force increases. All specimens were cleaned in an ultrasonic bath of acetone and dried. Before experiment, specimen surface roughness is measured. The average surface roughness (R_a) of the tube and the spring specimen is 0.76 μm and 0.67 μm, respectively.

Wear tester

Fig. 2 shows the schematic view of the wear tester and the tube specimen used for the present experiment. Servomotor, eccentric cylinder and lever are used to produce an oscillation of the tube specimen. The oscillation amplitude and frequency, which are measured using LVDT and FFT, can be adjusted. Four spring specimens are attached to fixtures using quick-dry glue, which are aligned 90° among each other to form a cell as given also in Fig. 2. Since four springs are aligned perpendicularly to constitute a cell into which the tube is inserted, the number of contact point between the tube and the

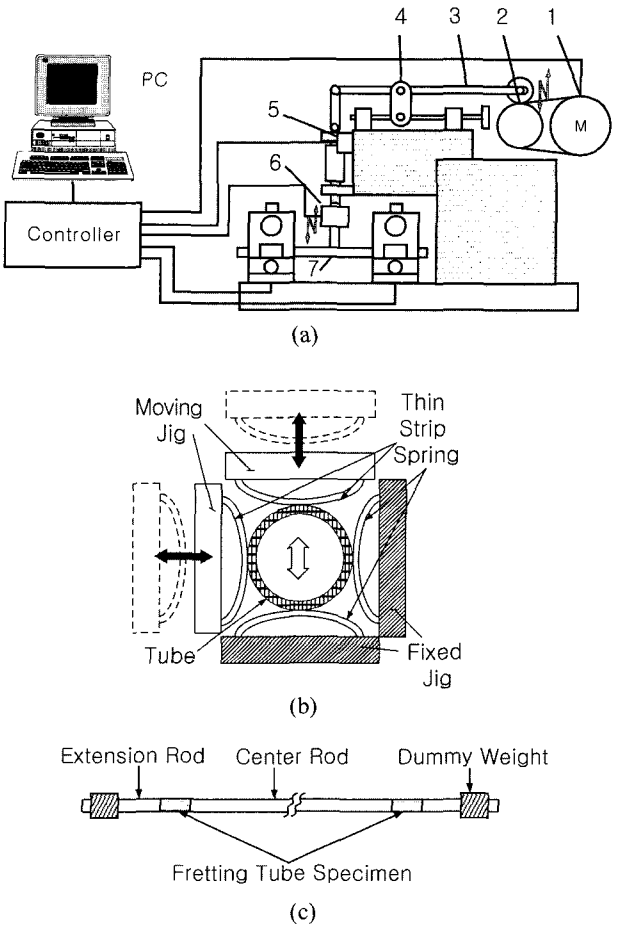

Fig. 2. Schematic diagram of the fretting wear tester and the configuration of the specimens (a) Fretting wear tester; 1: Servo-Motor, 2: Eccentric Cylinder, 3: Lever, 4: Movable Hinge, 5: LVDT, 6: Load Cell, 7: Tube Specimen (b) Contact configuration of the tube and the thin strip spring in a cell (c) Tube specimen assembly

spring in a cell is four. The tube specimen is inserted into two cells that locate at both left and right hand sides of the tube. The distance between each cell is set 522 mm that is the actual distance between the adjacent spacer grids in a nuclear fuel assembly. Two of the four spring fixtures of a cell are movable that enables the supporting condition of 5 N, just contact and 0.1 mm gap. Therefore, load cells are equipped inside the rest two stationary fixtures and dial indicators are installed on the movable fixtures of each cell.

Experiment method

Fretting wear experiment is performed under laboratory environment. Although the initial contact condition between the fuel rod and the spacer grid is intact (i.e., there is an adequate contact force, usually in the range of about 20~50 N), the contact force decreases due to thermal and irradiation effect in the reactor. At first, a comparatively small contact normal force of 5 N is applied to one of the three different contact conditions. From the condition of 5 N, the force is reduced by reversing the two movable fixtures (see Fig. 2(b)) at each cell

to obtain the condition of 0 N (just contact), which is the second condition in the experiment. Further reversing of the movable fixtures enables the last, 0.1 mm gap, condition. The adjustment is carried out using the load cell signal and the dial indicator.

The center rod of the tube specimen (see Fig. 2(c)) is connected to the rod fixture that oscillates up and down by the lever system. The frequency of oscillation is set 30 Hz and the range of it is 0.7 mm. Each experiment finishes when the oscillation cycle reaches 10^6. After finishing each experiment, the shape and dimension of wear scars on the two tubes (left and right hand side) are examined by a measuring microscope. A surface roughness tester is used to obtain the traces of the wear contour, which are logged while a stylus passes through on the scar. The maximum depth of wear is obtained from the traces. Wear volume is finally evaluated from the traces using a developed program [1]. The experiment is repeated three times for each condition.

Experimental Results and Discussions

Wear scar observation

Present contact configuration between the tube and the spring is a typical non-conformal contact since the spring has a convex contour in both axial and transverse direction, and the tube has a flat and a convex contour in axial and transverse direction, respectively. Contact length and width increase corresponding to the increase of normal contact force. Therefore, it may be regarded that a wear region becomes larger as the force increases under the same condition of vibration. However, this is valid when the whole contact region slips (gross slip). Under partial slip regime, the contact region is divided into central stick and outer slip region. Since wear occurs in the slip region, the prevailed slip regime can be readily estimated from the wear scar view. In general, wear becomes severer when the gross slip prevails. Therefore, it is important to know the slip regime to predict the severity of wear.

The slip regime depends on the contact normal force and slip displacement. The relation between them yields so-called "fretting map" [2]. Following the previous research on the fretting map, the partial slip is constituted when the force increases and the slip displacement decreases. As the force increases, the region of partial slip expands with the increase of the slip displacement. Moreover, it has been found that the boundary of partial and gross slip depends on the contact shape (i.e., the end profile of the contacting bodies). The partial slip region expanded in the case of contact between the tube and spring like the present case compared with the conventional ball on flat contact [3].

In the present experiment, the maximum force is 5 N. So, it is regarded *a priori* that the range of the slip displacement is less than 15 μm if the partial slip prevails according to the obtained fretting map [3]. The slip displacement on contact cannot be measured directly by the present wear tester. However, from the observation of the worn surface, gross slip always occurs as typically shown in Fig. 4. So it is concluded that the slip range on the contact is larger than 15 μm since the range certainly increases as the contact force decreases and in the case of gap existence.

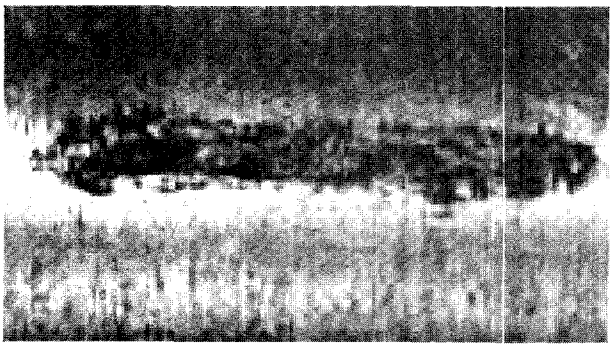

Fig. 3. Typical wear shape on the tube induced by the contact with the present thin strip spring (showing gross slip).

Influence of supporting condition on wear

Fig. 4 shows the wear volume and maximum depth of the wear on the tube specimen. Since a cell is composed of four springs, there are four wear scars on a tube specimen. So in total, eight wear scars are obtained for each experiment. As aforementioned, experiment is conducted three times for each condition. The maximum depth is obtained from eight wear scars for one supporting condition. While, the wear volume at each wear scar is summed altogether.

It is found that the wear volume decreases as the contacting force decreases. It is the smallest in the case of gap existence.

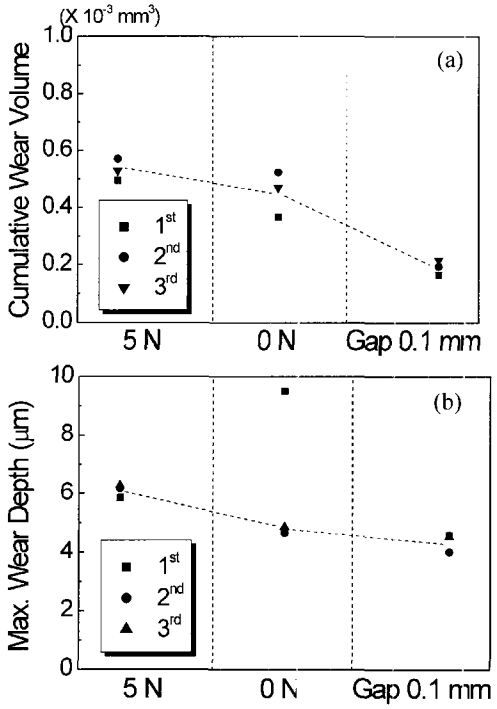

Fig. 4. Wear results corresponding to the different supporting conditions (a) Cumulative wear volume (b) Maximum wear depth.

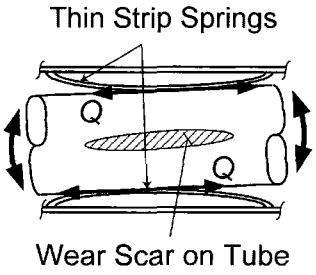

Fig. 5. Supposed tube motion during vibration.

This trend is also found in the plot of wear depth except the data at just contact condition of the first experiment. So, it is thought that the positive normal force yields severe wear in the case of present tube to spring contact. It is contrary to our expectation. In the case of positive contact (i.e., present 5 N and 0 N inclusive), we can expect a sliding contact between the tube and spring. While in the case of 0.1 mm gap, impacting is added to sliding. It is thought that an energy input to the system of contact is larger in the case of sliding and impacting than that of sliding only. So it is generally accepted that wear becomes severer if impacting is applied in addition to the sliding. However, it may be noted that the explanation is true if the tangential component of the force and displacement induced by the impacting is comparatively large since the wear is likely to occur by shear rather than normal force [4]. Therefore, the tangential (shear) component of the impacting force is regarded small in the present case of 0.1 mm gap. It may be explained from the contact shape and configuration of the present specimens.

When the center rod vibrates up and down reciprocally in the case of positive contact, the contact configuration inside the cell is as what is depicted in Fig. 5. So to speak, the tube inside the cell is repeatedly tilted. There occurs slip and wear on the contact during the repeated tilting. We anticipate the wear scar has the shape of being scrubbed along the tube axes (axial and transverse). This phenomenon is expected to decrease as the contact force decreases. It is thought to disappear when the normal force is zero. In the case of gap existence, however, it is expected that the phenomenon appears to some extent since a positive contact force occurs during impacting. As the surface is scrubbed, wear occurs. It can be said that the severity of the wear depends on the force of scrubbing, which is equivalent to the tangential force on the contact. This can explain the less substantial wear in the case of 0.1 mm gap compared with the wear in the case of 5 N. The above phenomenon can be examined by detail observation of the worn surface. It is conducted using SEM in the present study.

SEM observation of the wear scar

Detailed examination of the worn surface using SEM is given in Fig. 6. In this figure, the upper row shows the worn surface observed on the tube at the locations of either upper or lower spring fixture (refer to Fig. 2 (b)), which is regarded to occur due to axial slip. While the lower row in Fig. 6 shows the worn surface at the locations of either left or right spring fixture (refer to Fig. 2 (b)), which is regarded to occur due to transverse slip. The results for the contact force of 5 N, 0 N and 0.1 mm gap conditions are given from left to right in the upper and lower rows of Fig. 6.

Wear in the case of axial slip is considered at first. In the case of 5 N, plastic flow is apparently seen. The wear mechanism is, therefore, the plastic deformation and resultant detachment of deformed asperities. However, the plastic flow is not found in the case of just contact. Flat deformed layer is

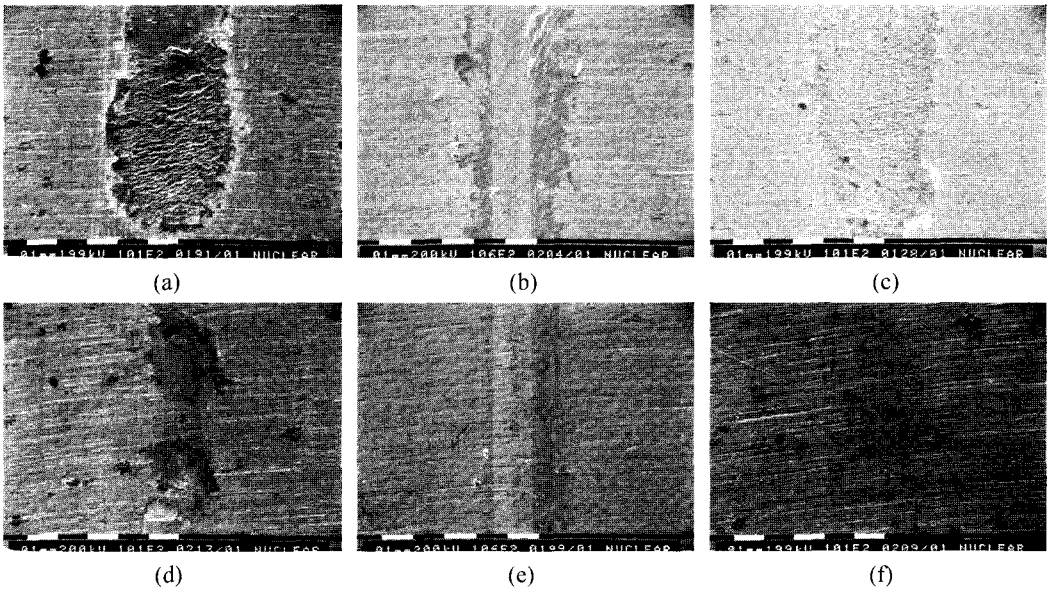

Fig. 6. Detail observation of the worn surfaces by SEM; upper row (axial) shows the wear at upper and lower contact positions and lower row (transverse) shows the wear at left and right contact positions in Fig. 2(b) (a) P = 5 N, axial (b) P = 0 N, axial (c) Gap 0.1 mm, axial (c) P = 5 N, transverse (d) P = 0 N, transverse (e) Gap 0.1 mm, transverse.

found together with fine debris. In the case of 0.1 mm gap, the plastic flow is observed again but the severity is less than the case of 5 N. Therefore, in the case of 5 N, relatively larger deformation and wider region of wear debris produced result in relatively larger and thicker wear debris compared with the other two conditions. In the case of 0.1 mm gap, the plastic deformation is not large.

The plastic flow can also be explained from the smooth spring contour and the contact angle (the angle between the radial direction of the tube and the normal direction to the spring surface) at the time of impacting. The contact angle is thought small at the time of impacting (due to tilting of the tube), which results in the tangential component of the contacting force being small. In this case, the capability of debris producing can be less than that in the case of plain rubbing which is the case of just contact. However, it cannot be true if the spring of different contact shape is used. For instance, if the spring has a flat contour with respect to the tube axis, the contact angle increases, and possible high stress at the edges may result in further severe wear in the case of gap existence.

On the other hand, wear is found much less in the case of transverse slip as shown in the lower row of Fig. 6. Further, it is hard to distinguish the wear scar from the intrinsic scratches on the tube in the cases of just contact and 0.1 mm gap. The plastic deformation is hardly found even in the case of 5 N. This implies that the wear mechanism is different depending on the slip direction. From our experimental results, the axial slip should be considered more intensively in the case of present contact configuration.

Contact Traction Analysis

Contact mechanics theory

Since wear is primarily caused by shear on the contact surface, the evaluation of the contact traction may give an idea of wear prediction. The contact shape affects the contact traction. For instance, if the traction is high at the contact edges seen in the case of square ended indenter, severe wear occurs at and around the contact boundary. If a ball or a cylinder indents a flat surface, semi-ellipsoidal traction profile is generated (i.e., the Hertz pressure). Partial slip regime in the case of the Hertz contact yields the worn area of annulus shape. The above solutions of the traction are well provided in the field of contact mechanics [5,6]. General solution of the traction in two dimensional problem is evaluated from the following coupled singular integral equations with the assumption of the contacting bodies being semi-infinite, in other words, the contact region is small compared with the characteristic dimensions of the bodies. Therefore, a non-conformal contact problem is usually dealt with in contact mechanics.

$$\frac{E^*}{2}\frac{dh(x)}{dx} = \frac{1}{\pi}\int_{-b}^{b}\frac{p(\eta)}{x-\eta}d\eta - \beta q(x), \tag{1}$$

$$\frac{E^*}{2}\frac{dg(x)}{dx} = \frac{1}{\pi}\int_{-b}^{b}\frac{q(\eta)}{x-\eta}d\eta + \beta p(x) \tag{2}$$

where, $h(x)$ and $g(x)$ are normal and shear tractions, respectively. b is a half of the contact length. E^* and β are defined as

$$\frac{1}{E^*} = \frac{(1-\nu_1^2)}{E_1} + \frac{(1-\nu_2^2)}{E_2}, \tag{3}$$

$$\beta = \frac{1}{2}\left[\frac{\{(1-2\nu_1)/G_1\} - \{(1-2\nu_2)/G_2\}}{\{(1-\nu_1)/G_1\} + \{(1-\nu_2)/G_2\}}\right] \tag{4}$$

where, the subscripts 1 and 2 designate the two different bodies in contact. E and G are the elastic and shear modulus, respectively. ν is the Poisson ratio. In the present case, $\beta = 0$ since the material of the spring and the tube are the same.

The semi-infiniteness cannot be assumed for the present problem although it is non-conformal contact since the thickness of the spring and the tube is even smaller than the contact length, which is thought equivalent to the wear scar length. Therefore, Eqs. (1) and (2) cannot be applied directly, and other method such as the Fourier transform analysis or the finite element method may be consulted. In the present study, the latter is used for obtaining the traction. Another purpose of the traction analysis is to investigate the change of traction profile, which may occur probably as the contact force increases and the contact shape is altered considerably. This is concerned especially in the case of the contact with thin strip like the present problem.

Finite element analysis

Verification of finite element implementation

For the finite element analysis, the commercial codes I-DEAS (version 8) and ABAQUS (version 5.1) are used. The former is used for shape modelling, while the latter for analysis. Four-node shell elements are used for the spring. The tube is modeled as a rigid cylinder whose diameter is 9.5 mm, the outer diameter of the tube specimen. Elastoplastic analysis is carried out to accommodate the local plastic deformation probably produced in the spring during the application of the force by the rigid cylinder. As for the mechanical properties of the spring, the values in Table 1 are used. Modelling the tube as a rigid cylinder is for easy implementation of the element. It is expected that the traction profile and the size of the contact region may be altered a little if we implement an actual elastic tube rather than a rigid cylinder. This is because only the

Table 2. Number of elements used in different meshes

	Total	Top region
Mesh I	1970	40 × 3
Mesh II	4119	80 × 5
Mesh III	11609	200 × 10

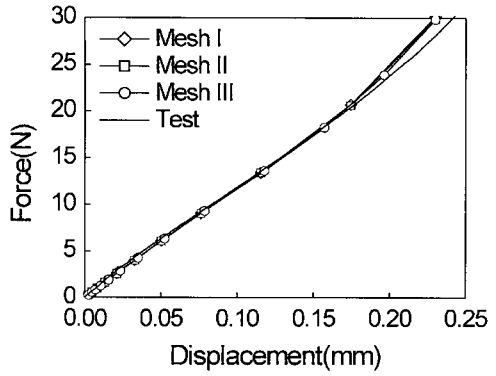

Fig. 7. Verification of present FE analysis by comparing with the test curve of the spring characteristic.

elastic constant E^* is to be changed in Eqs. (1) and (2), which does not affect the form of the equations. With respect to the coordinate system in Fig. 1, displacement in the y-direction and rotation about x- and z-directions are constrained at both ends in the x-axis for the boundary condition. Additionally, displacement in the y-direction and rotation about z-direction are constrained at the side, distant from the end of the spring by 0.4 mm, which is clamped in the spacer grid assembly.

To verify the modelling and the analysis method, the relationship between the force and the displacement of the spring (i.e., *characteristic curve*) is benchmarked. At first, the influence of the element size is checked. To this end, three different finite element meshes are used as demonstrated in Table 2. The second column of Table 2 designates the total number of elements of spring and the last column shows the number of elements of the imposed contact region (10 mm × 0.5 mm) of the spring. Fig. 7 shows the result up to the force of 30 N that is designed for the present spring force. It is seen that the characteristic curves obtained from finite element analysis agree well with the test result. We can conclude that the present finite element implementation of the deformation of the spring is verified regardless of the number of elements.

Secondly, contact traction is evaluated with the three different meshes when the spring is pressed by 0.15 mm. As shown in Fig. 8(a), different traction (pressure) values appear corresponding to the number of element. As the number of elements increase, traction increases considerably. This implies that the contact region decreases as the number of element increases (in other words, as the element size decreases), because the contact forces are almost the same regardless of the number of elements as shown in Fig. 7. It seems to be caused by a line contact that is regarded to form in the present contact configuration (i.e., contact of convex contours in transverse direction). So to speak, the contact width calculated by the finite element method becomes further narrower as the element width decreases. However, if we non-dimensionalize the traction with respect to the average traction like below, an almost similar traction is obtained regardless of the element size (number) as given in Fig. 8(b).

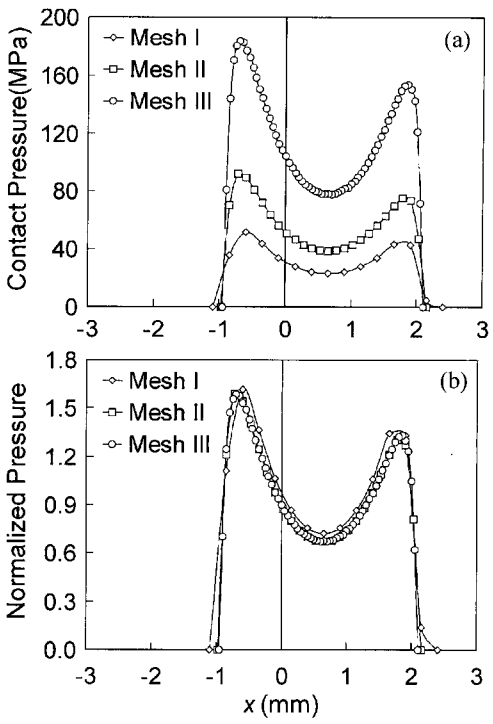

Fig. 8. Contact pressure distribution obtained by FEM with different meshes (a) Direct result of the contact traction obtained by FEM (b) Normalized contact traction of (a) with respect to the average pressure.

$$\bar{p}_i = \frac{p_i}{p_0} = \frac{p_i}{P/A} \tag{5}$$

where, p_i is the non-dimensionalized normal traction, p_i is the traction at each nodal point and p_0 is the average traction. P is the contact normal force and A is the area of the contact region evaluated during the analysis with ABAQUS.

Because the intrinsic purpose of present finite element method to obtain the contact traction is to investigate the change in traction profile during the force increase, the above matter is not considered further in detail. Nevertheless, it should be kept in mind that a special care is necessary during designing the element size in finite element method to deal with this kind of line contact problem. For the rest of the analysis, the smallest element size (Mesh III) is used to obtain a large number of data in the contact region and the non-dimensionalized traction, p_i is investigated. On the other hand, we can expect the supposed change in traction profile, since Fig. 8 is considerably different from the profile of the Hertz pressure (semi-ellipsoidal shape) which may well occur when the spring starts to be pressed by the solid cylinder.

Analysis results and discussions

Fig. 9 shows the progress of deformation of the spring top surface as it is pressed down by up to 0.15 mm. The contact region is depicted with solid marks. The deformed shape and

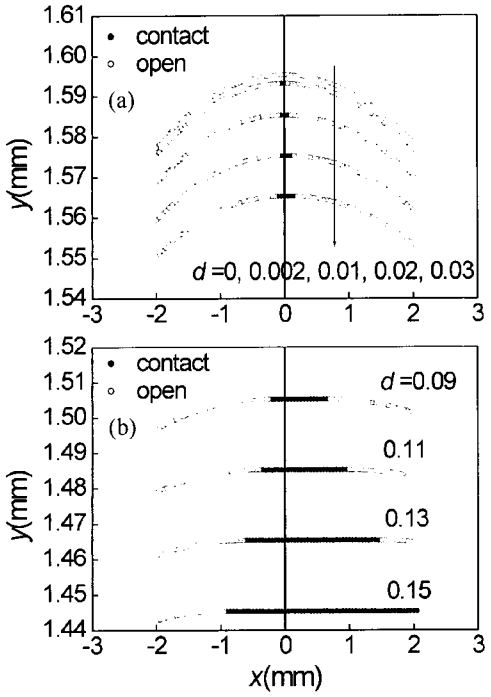

Fig. 9. Deformed shape and contact region during the increase of contact force (a) Compressive displacement, d = 0~0.03 mm (b) Compressive displacement, d = 0.09~0.15 mm.

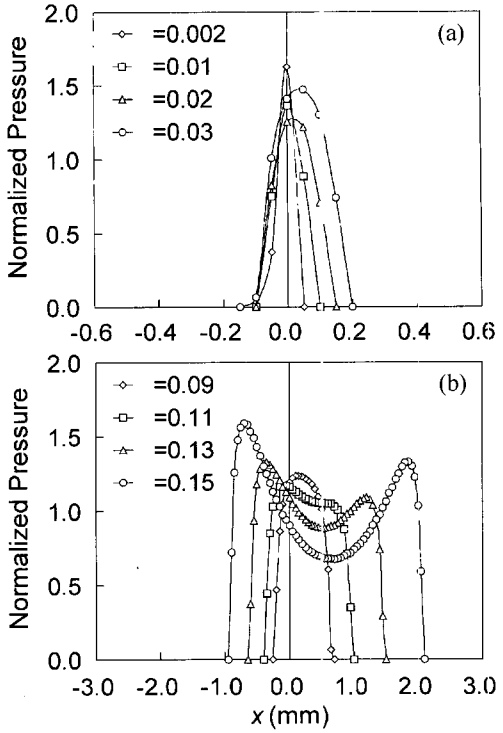

Fig. 10. Variation of contact traction profile during the increase of contact force (corresponding to Fig. 9) (a) Compressive displacement, d = 0.002~0.03 mm (b) Compressive displacement, d = 0.09~0.15 mm.

the expansion of the contact region are shown well. As has been expected, the shape of the contact region is shown flat and the length of it increases following the compressive displacement. Fig. 10 gives the contact normal traction evaluated corresponding to the displacements in Fig. 9. Until the spring is pressed by 0.09 mm, the traction profile is similar to the Hertzian (higher traction at the central region of the contact). However, if the spring is pressed further, the traction of central region becomes smaller than that of the region near contact boundary. It seems to be similar to the traction induced by the indentation of a punch with rounded edges [3].

It is thought reasonable at the moment that the traction profile resembles that of the punch with rounded edges in shape since the central flat and the outer curvature regions of the deformed spring shape is similar to the end profile of the punch with rounded edges. However, it should be noted that such a condition is valid when the contact boundary locates within the region of the curvature region. In other words, the spring itself should deform elastically in the direction of thickness. Unfortunately, this cannot be examined in detail from the present finite element analysis since the general shell element used for the spring cannot represent the deformation in the direction of thickness. This work is remained for further study.

Nevertheless, it is apparent that the traction profile is altered during the force increase. This implies that the location of wear concentration is altered depending on the contacting force that is directly related with the compressive displacement of the spring. At the beginning of fuel life, the spring is intact and has the design force. As the residence period in the reactor increases, the spring force decreases not only by the degradation of the spring stiffness but also by the decrease of fuel rod diameter due to creep down. In this case, the location of wear may be moved from contact boundary to the center of the spring where the higher traction occurs. From Figs. 7 and 10, it can be regarded that the contact traction in the present experiment is similar to the Hertzian since the maximum force was 5 N, at which the displacement is $\approx$ 0.035 mm.

Concluding Remarks

In this study, wear of a vibrating tube supported by thin strip springs in the case of various supporting conditions is analyzed experimentally. As for the influence of the supporting condition on the wear severity, it is found that the wear volume increases in the order of the 0.1 mm gap, the just contact and the 5 N conditions. This is explained from the contact shape of the present spring, which has convex and smooth contour because the contact region expands following the applied normal force. The contact shape also affects the wear mechanism. SEM observation shows the plastic flow on the tube surface apparently in the case of 5 N. While, it is found less in the case of gap existence, and disappears at the just contact case. Contact angle, defined as the angle between the radial direction of the tube and the normal direction to the spring surface, is considered to explain the observed plastic flow, which is also determined by the contact shape. All the worn surfaces reveal gross slip. Finite element analysis gives

the contact traction in the experiment is similar to the Hertz pressure. Therefore, it is regarded that the slip displacement on the contact is larger than 15 μm with consulting the previously presented fretting map [2,3]. On the other hand, it is found that the shape of the contact traction profile changes as the contact force increases. This implies that the wear location can be altered during the residence period of nuclear fuel inside the reactor. This work needs further study since it is closely related with the spring design in the point of wear restraining. Present work is primarily concerned with the contact and wear problem of nuclear fuel and spacer grid. But it is not limited to that subject, it can be applied to a further general wear and contact problem of thin strip structures.

Acknowledgment

This work has been carried out under the Nuclear R&D Program by Ministry of Science and Technology in Korea.

References

1. Kim, H.-K. and Kim, S.-J., Development of Algorithm for Wear Volume Evaluation using Surface Profile Analysis, J. Kor. Soc. Tribologists and Lubr. Engrs., Vol. 17, No. 1, pp. 33-39, 2001.
2. Fouvry, S., Kapsa, P. and Vincent, L., Quantification of Fretting Damage, Wear, Vol. 200, pp. 186-205, 1996.
3. Kim, H.-K., Kang, H.-S. and Song, K.-N., The Influence of Contact Shape on the Slip Regime in Contact-induced Failure, KSTLE Int. J., Vol. 2, No. 2, pp. 85-92, 2001.
4. Ko, P.L., The Significance of Shear and Normal Force Components on Tube Wear due to Fretting and Periodic Impacting, Wear, Vol. 106, pp. 261-281, 1985.
5. Hills, D.A., Nowell, D. and Sackfield, A., Mechanics of Elastic Contacts, Chap. 2, pp. 45-61, Butterworth-Heinemann, Great Britain, 1993.
6. Johnson, K.L., Contact Mechanics, Chap. 2, pp. 18-35, Cambridge Univ. Press, Great Britain, 1985.